International Journal of Technology (2016) 2: 306-313
ISSN 2086-9614 

# THE EFFECT OF PLASMA ACTUATOR PLACEMENT ON DRAG COEFFICIENT REDUCTION OF AHMED BODY AS AN AERODYNAMIC MODEL

James Julian[2], Harinaldi[1*], Budiarso[1], Revan Difitro[2], Parker Stefan[2]

[1] *Departement of Mechanical Engineering, Faculty of Engineering, Universitas Indonesia, Kampus UI Depok, Depok 16424, Indonesia*
[2] *Fluid Mechanics Laboratory, Departement of Mechanical Engineering, Faculty of Engineering, Universitas Indonesia, Kampus UI Depok, Depok 16424, Indonesia*

(Received: October 2015 / Revised: December 2015 / Accepted: January 2016)

## ABSTRACT

In recent developments in the area of thermofluid technologies, active flow control has emerged as an interesting topic of research. One of the latest methods, which will be discussed in this paper, is the application of a plasma actuator. Plasma actuation is achieved by conducting a high-voltage electric current through an actuator device. Our research was specifically conducted to discover its effect on the reduction of the drag coefficient, with Ahmed Body the experimental object put inside a suction-flow wind tunnel with varying inputs of flow velocity. The plasma actuator device was run with an A.C. power supply and installed in three different placement configurations on the aerodynamic model to determine which most optimally affected the aerodynamic drag, while the drag coefficients were acquired via the use of a load cell installed as the harness for the aerodynamic model inside the tunnel. The results of the experiments include that the optimal configuration of the actuator placement was on the leading edge, the optimal wind flow velocity of the experiment, which was essential for the actuation to be observed, was at 1.7 m/s, and the resulting drag reduction percentage, as a result of induced flow, was 22% of the initial drag coefficient.

*Keywords:* Active flow controls; Ahmed body; Drag reduction; Plasma actuator

## 1. INTRODUCTION

A number of aerodynamic studies have been conducted on four-wheeled vehicles in order to determine the contributory effect of fuel consumption (Indonesia Energy Outlook, 2012). There are many forces that work on a vehicle, one of which is called *drag*, which is described as an aerodynamic force working in the opposite direction to a moving object that creates flow separation around the geometry of the vehicle. This drag force leads to the generation of pressure differences and the formation of vortex shedding, otherwise known as *pressure drag*, which is a part of *form drag*. This phenomenon may cause extra work for the engines and excessive consumption of fuel. Recent advances in aerodynamic studies have introduced a concept of manipulating air flow around an object to reduce drag coefficient in a vehicle. This is divided into two control schemes: *passive control* (modifying the geometry of an object) and *active control* (manipulating the dynamics of air flow around the object).

Passive control schemes involve turbulent flow generation, as well as the installation of a modification of low interchangeability, producing less satisfying research parameters and

*Corresponding author's email: harinald@eng.ui.ac.id, Tel. +62-21-7270032, Fax. +62-21-7270033
Permalink/DOI: http://dx.doi.org/10.14716/ijtech.v7i2.2994

results (Harinaldi et al., 2015). In contrast, active flow control involves transition delay by altering the shape of the velocity profile to minimize unstable wave growth, elimination of disturbances from superposition of vibrations, and boundary layer separation control by applying either a suction or blowing scheme to an external flow (Gad-El-Hak et al., 1998). An active control scheme using *plasma actuation* is one of the latest efforts to reduce fuel usage in vehicles. A particular object called an *Ahmed Body* has been widely utilized as a simplified vehicle model for aerodynamic testing purposes; it displays external flow conditions that bear adequate comparison with a real vehicle model (Ahmed et al., 1984)**.** In the past, researches have been conducted on wake flow and turbulence analysis at the rear side of the Ahmed body at an inclined angle of $25^o$ to $35^o$. Such experiments progressed further by applying a flow diagnostic using a laser doppler anemometer, as well as in a computational manner using a modified arge eddy simulation (Tarakka, 2012).

The objective of this experiment was to determine the effect of plasma induction on an aerodynamic model, specifically an Ahmed body, utilizing variation of actuator placement on the leading edge, trailing edge, or both the leading and trailing edges of the model. Another objective was to gain a deeper understanding of plasma induction and its effect in advancing the research on this particular field of active flow control in aerodynamic studies. The data acquired from the research can then provide a reference for computational method study in the same field.

## 2. METHODOLOGY

The research was focused on observing the external flow surrounding an aerodynamic body while it is being induced by a plasma actuator. The experiment was conducted by utilizing an aerodynamic object called an Ahmed Body, as shown in Figure 1, with a 1:4 scale and an inclined trailing edge at $30^o$ in a suction-flow wind tunnel capable of delivering airflow at a velocity of 16.7 m/s.

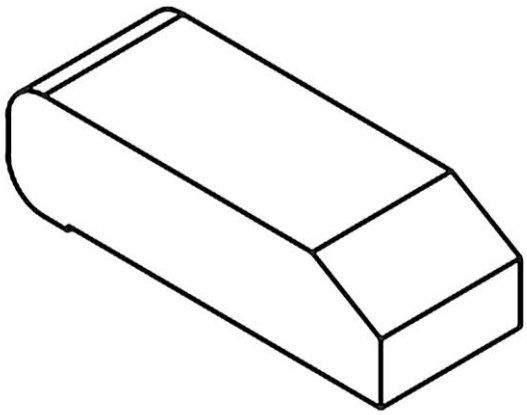

Figure 1 Isometric projection of an Ahmed Body model

The object was installed with a *Single Dielectric Barrier Discharge* (SDBD) plasma actuator, an electric device shown in Figure 2 that consists of two electrodes made from either thin copper or aluminum plate and separated by a dielectric that induces the air around the object, transforming the trajectory of the flow as well as streamlining the boundary layer. The selection of dielectric material was crucial, as it would affect the device's toughness against electric resistance. The upper electrode contains positive charges, while the lower electrode works as the ground, and is either submerged into the dielectric or exposed to air. Electric discharge flows downstream along the dielectric, and the presence of the dielectric negates any short circuit that might happen in a surge. An induction of plasma occurs by applying a high-voltage

current to an electrode, and the different polarity between the plasma (+) and open air (-) causes magnetic attraction that leads the airflow onto the plasma.

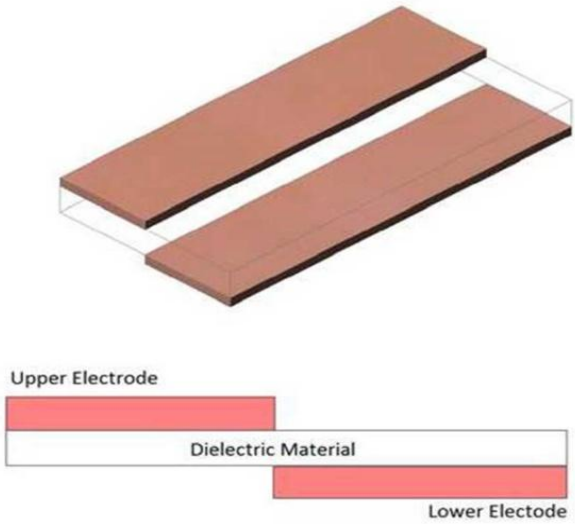


Figure 2 Plasma actuator device

Parameters were observed to prove that the presence of the actuation is the drag coefficient. There are three different configurations of actuator position as shown in Figure 3; namely, leading edge, trailing edge, and leading and trailing edge. The wind tunnel was activated with varying velocities of suction flow: 1.7 m/s, 4.3 m/s, and 6.3 m/s. The drag coefficient was acquired via the use of a load cell installed inside the aerodynamic body. The governing equation of the drag ($D$) is written as:

$$D = \frac{1}{2}\rho V^2 A C_D \quad (1)$$

In which;

$C_D$ : Drag coefficient
$\frac{1}{2}\rho V^2$ : Free stream dynamic pressure (Pa)
$A$ : Characteristic area ($m^2$)

The experimental data acquired would then be presented in the form of a two-dimensional graph of drag coefficient vs time, with variables provided from the actuation of plasma.

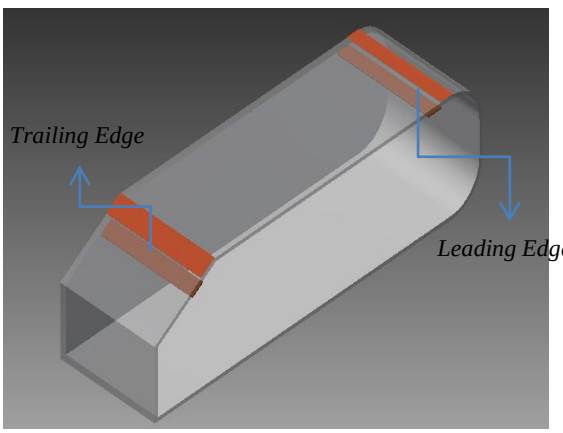


Figure 3 Actuator placement on the model

The experiment was conducted inside a suction-type wind tunnel, as shown in Figure 4. The wind tunnel was 260 cm long, with a 55 cm tip diameter. Flow was generated by an axial blower utilizing a 1.5 kW D.C. motor rotating at 2800 rpm. The tunnel was equipped with an additional honeycomb mesh to straighten the wind flow. Free stream flow was measured with a hot wire anemometer. The test model was placed in a section located in the middle of the tunnel, where data acquisition took place. An electrical setup was then assembled to power the plasma actuator, as shown in Figure 5.

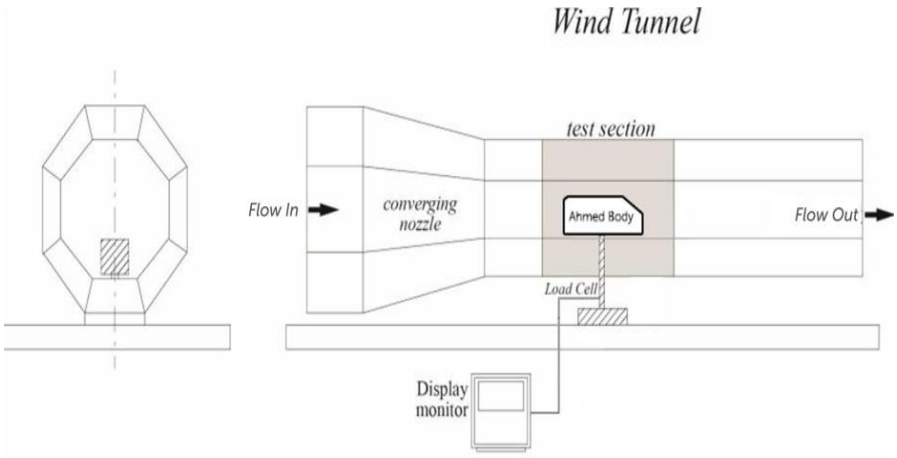


Figure 4 Wind tunnel setup

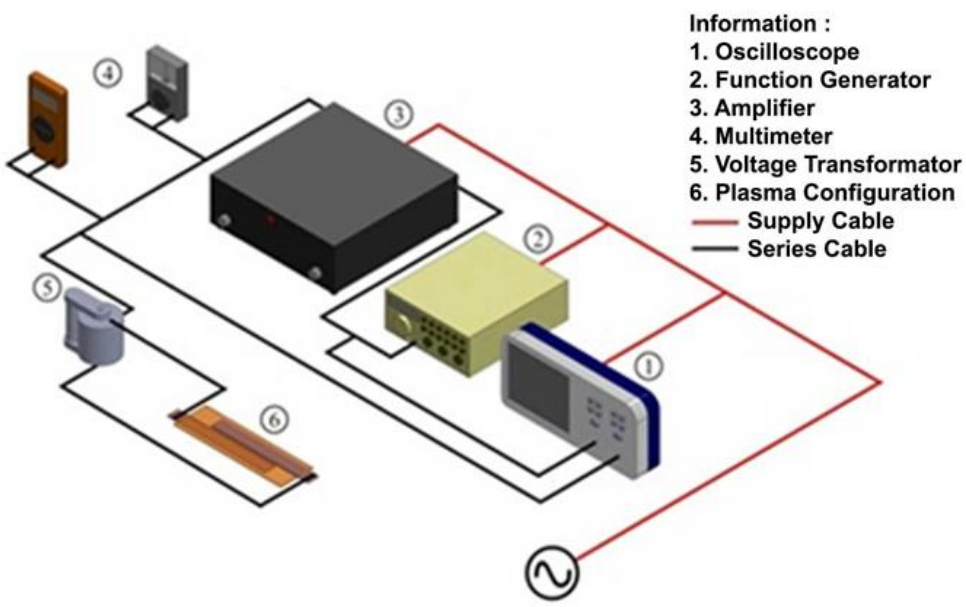


Figure 5 Electrical devices setup schematic

Its main component was the function generator that generated square-form waves with a frequency of 9 kHz. The signal was then transmitted with an amplifier and increased through a step-up transformer capable of 11000 $V_{p\text{-}p}$ in gain, which was used to power the dielectric.

The voltage had to be kept stable at 40 V, in order for the dielectric to actuate plasma of good quality. Two types of multimeters were used. An analog meter was placed between the fuse and amplifier, and a digital one was placed between the fuse and transformer. This was done so that

electric current disturbance, as well as fuse breakage, could be detected. Finally, an oscilloscope was installed to monitor the signal transmission.

## 3. RESULT AND DISCUSSION

The experiment yielded results. Numerical data was obtained over time and then processed and presented in graphical form, divided into nine different charts with different actuator configuration over inputs of free stream flow speed. Data acquired by observing the fluctuation in the load cell for 120 seconds was converted into drag force and further observed to identify the upper and lower boundaries of the load cell reading. The following is the experimental data acquired with differing configurations of actuator placement and varying free stream velocity.

Drag forces acquired from the experiment differed with each reading. A higher free stream flow speed resulted in more fluctuation in the acquired data since the flow was highly likely to be turbulent; therefore, fluid particles would not follow the contour of the model, resulting in faster generation of separation.

Plasma induction worked to prevent such phenomena from happening by manipulating the occurrence of separation and forcing the flow profile to follow the model contour. As a result, the wake behind slipped and was weakened, causing a smaller pressure difference between the front and back of the model and decreasing the drag force.

Figures 6 to 8 show the effect of the leading edge configuration over three different free stream speeds. The best result for drag reduction is shown in Figure 6, when the free stream was at 1.7 m/s, expressed by a stable value of 7 N from 9 N over 120 seconds when the actuator was active. Figure 7 shows slightly fluctuating numbers, averaging at 55.20 N, which reduced drag force from 57.36 N. Figure 8 shows great fluctuation in the numbers at a 6.3 m/s flow speed, which averaged at 118.48 N, reducing drag force from 121.92 N.

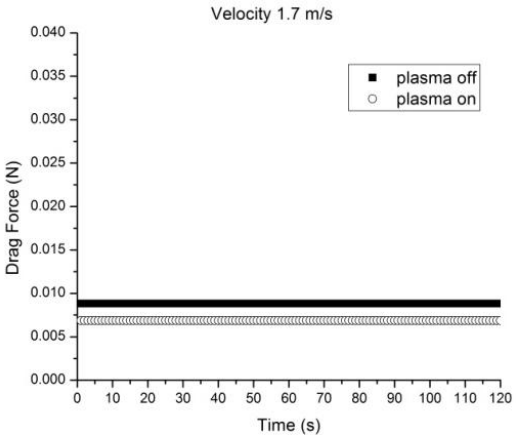


Figure 6 Drag force vs time for leading edge configuration at 1.7 m/s flow speed

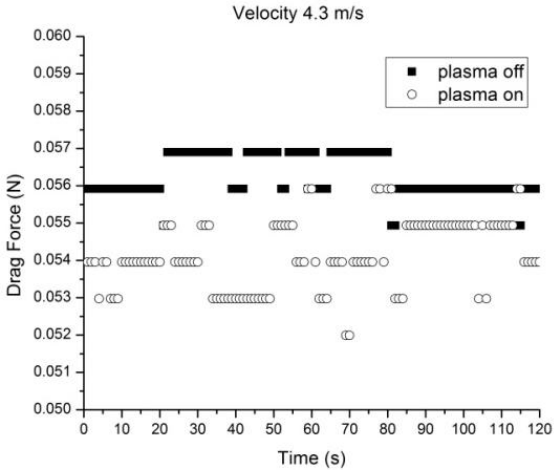


Figure 7 Drag force vs time for leading edge Configuration at 4.3 m/s flow speed

Figures 9 to 11 display the results for the trailing edge configuration. These are negative results, with a decreasing effect on the lower flow speed. The test with a 1.7 m/s free stream flow speed showed a reversed outcome, with the drag being increased, from an averaged amount of 9 N to 9.08 N. The test with a 4.3 m/s flow speed fared better, showing a reduced drag force of 57.36 N from 55.19 N, while the test with a 6.3 m/s flow speed showed a reduced force of 120.7 N from 118.45 N.

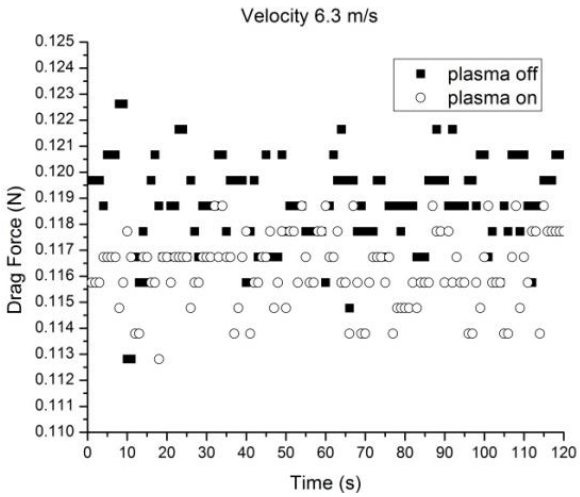


Figure 8 Drag force vs time for leading edge configuration at 6.3 m/s flow speed

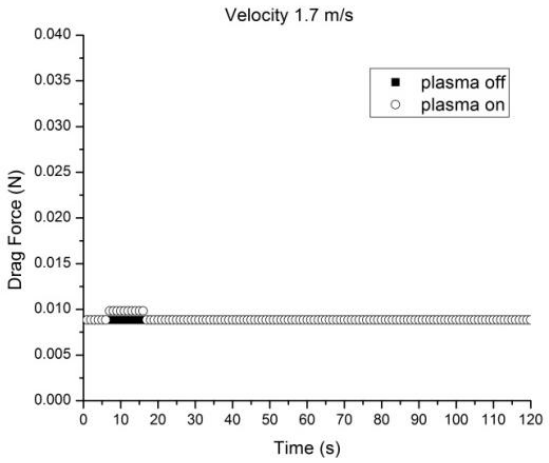


Figure 9 Drag force vs time for trailing edge configuration at 1.7 m/s flow speed

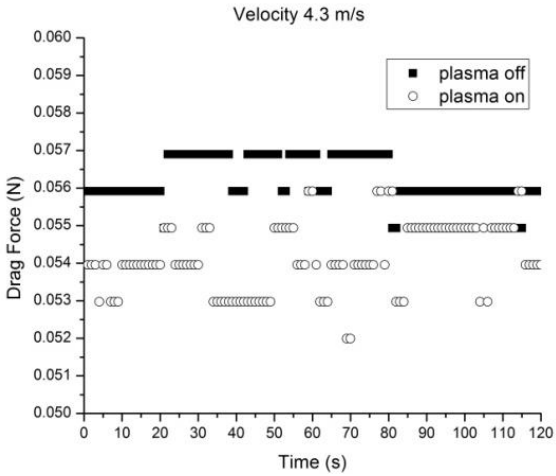


Figure 10 Drag force vs time for trailing edge configuration at 4.3 m/s flow speed

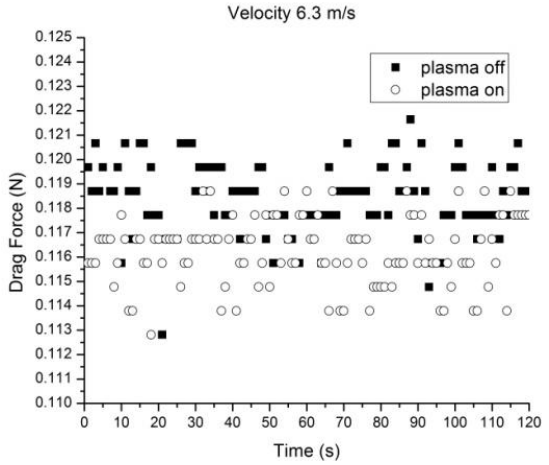


Figure 11 Drag force vs time for trailing edge configuration at 6.3 m/s flow speed

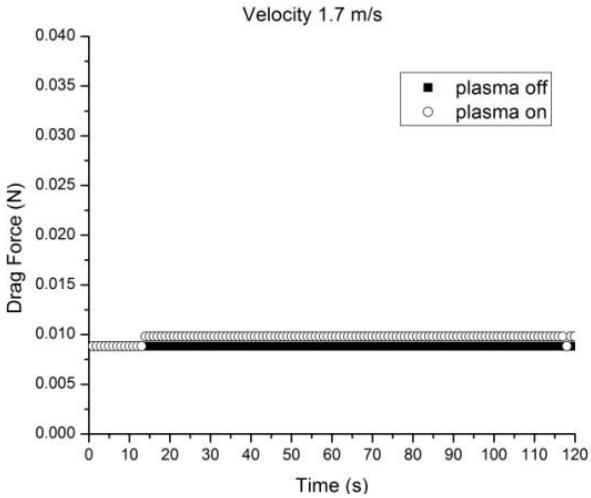


Figure 12 Drag force vs time for leading and trailing edge configuration at 1.7 m/s flow speed

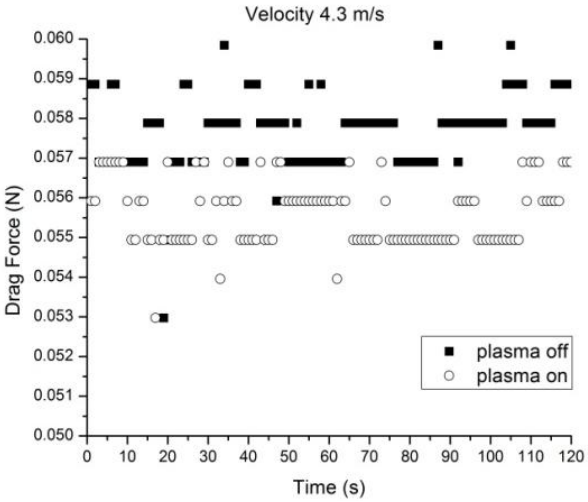


Figure 13 Drag force vs time for leading and trailing edge configuration at 4.3 m/s flow speed

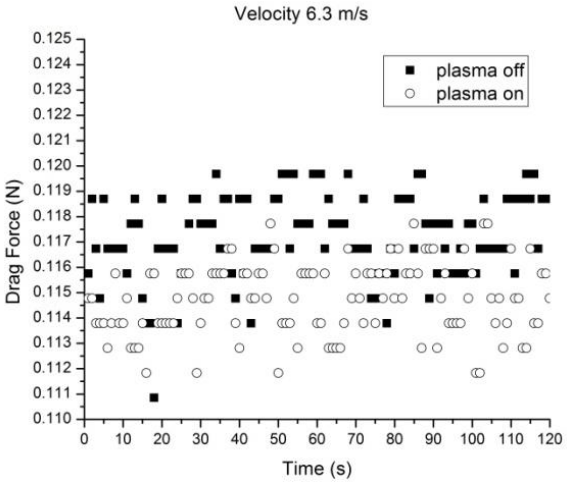


Figure 14 Drag force vs time for leading and trailing edge configuration at 6.3 m/s flow speed

Figures 12 to 14 display the results for a combination of leading and trailing edge configurations. The 1.7 m/s flow speed test yielded a reduction from 9 N to 8.1 N of drag force. The 4.3 m/s flow speed test yielded a reduction from 58.8 N to 56.66 N of force. The 6.3 m/s flow speed test yielded a better overall result, with a reduction from 119.5 N to 116.93 N of force.

Table 1 Drag reduction of the three configurations

| V (m/s) | Drag coefficient | | |
|---|---|---|---|
| | Leading edge configuration | Trailing edge configuration | Leading and trailing edge configuration |
| 1.7 | 22.40005242 | 0.048266703 | 15.0773617 |
| 4.3 | 5.429733842 | -0.920020231 | 4.529691298 |
| 6.3 | 3.226618581 | 2.912394073 | 4.723203326 |

From Table 1, it can be deduced that at a 1.7 m/s flow speed, when the actuator is placed on the leading edge, the maximum drag reduction occurred at a stable number of 2 N. A negative result occurred when the actuator was placed on the trailing edge at a 4.3 m/s flow speed, which instead of reducing the drag, ended up increasing it by 0.08 N. An analysis of which configuration performed the best can be seen in Figure 15 below.

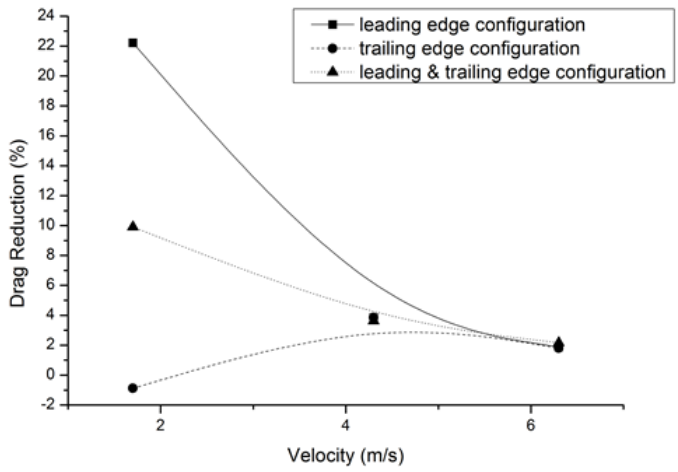


Figure 15 Drag reduction value over time

## 4. CONCLUSION

By analyzing the results, conclusions can be drawn regarding several parameters of the experiment. First, it was shown that utilizing a 1/137.5 step up voltage transformer to regulate the actuator power supply during the experiment induced the flow around the aerodynamic body, minimizing separation and, as a result, reducing the drag coefficient. The optimal position for the actuator placement was located at the leading edge of the aerodynamic body. It can be deduced that at low velocity, when free stream flow started hitting the model at the leading edge, the actuation immediately transformed the flow profile before separation could occur, rendering the placement of the actuator on the trailing edge ineffective; this explains why placing the actuator at the leading edge is the best course of action. However, at a higher flow speed, the actuation could no longer control the flow. Finally, several limitations were discovered; for example, when the 5 m/s free stream velocity test took place, the actuator could not reduce the drag by more than 5%. Our hypothesis is that the electrode material could not produce enough actuation to control the flow beyond the maximum flow speed used in the experiment.

## 5. REFERENCES

Ahmed, S., Ramm, G., Faltin, G., 1984. Some Salient Features of the Time-averaged Ground Vehicle Wake. *SAE Technical Paper 840300*, doi: 10.4271/840300

Anderson, J.D., 2001. *Fundamentals of Aerodynamics (3rd Ed). McGraw-Hill*, Singapore

Badan Pengkajian dan Penerapan Teknologi, 2012. Indonesia Energy Outlook 2012. *BPPT-Press*, Jakarta

Gad-El-Hak, M., Pollard, A., Bonnet, J.P., 1998. Flow Control Fundamentals and Practices. From Lecture Notes in Physics, *New Series m53: Monographs, Springer-Verlag*, Berlin Heidelberg

Harinaldi., Budiarso., Julian, J., Andika, W.S., 2015. Drag Degradation in Flow Separation using Plasma Actuation in Cylinder Model. *SNTTM XIV proceedings*, Banjarmasin, Indonesia

Tarakka, R., 2012. *Kajian Kontrol Aktif Aliran Separasi Aliran Turbulen pada Aerodinamika Bluff Body Model Kendaraan*. PhD Disertation, Department of Mechanical Engineering, Faculty of Engineering, Universitas Indonesia, Depok, Indonesia (in Bahasa)